Characterization of phorbol ester-stimulated serine phosphorylation of the human insulin receptor

Edward P. FEENER,* Teruo SHIBA, Kang-Quan HU, Peter A. WILDEN, Morris F. WHITE and George L. KING
Research Division, Joslin Diabetes Center, Department of Medicine, Brigham and Women's Hospital, Harvard Medical School, Boston, MA 02215, U.S.A.

Phorbol 12-myristate 13-acetate (PMA)-stimulated phosphorylation of the human insulin receptor (IR) was characterized and compared in two cell types of different lineage: normal rat kidney epithelial (NRK) cells and Chinese hamster ovary (CHO) fibroblasts. PMA stimulation increased IR β-subunit phosphorylation to 252 ± 43 and 259 ± 47% ($\pm$S.D.) of the unstimulated control in NRK and CHO cells respectively. Tryptic phosphopeptide analysis by Tricine/SDS/PAGE revealed significant differences in the PMA-stimulated phosphorylation of the IR in these two cell types. This phosphorylation of the IR was predominantly located in two tryptic phosphopeptides, and these phosphopeptides were absent in an IR mutant truncated by 43 C-terminal amino acids. The major PMA-stimulated tryptic phosphopeptide from *in vivo*-labelled CHO/IR was immunoprecipitated with an antibody against residues Ser^{1315} to Lys^{1329}, and this precipitation was blocked with excess unlabelled peptide containing this sequence. Radiosequencing by manual Edman degradation revealed that this tryptic phosphopeptide was phosphorylated at Ser^{1315}. This PMA-stimulated phosphorylation did not inhibit autophosphorylation of the IR *in vivo*. These results demonstrate that PMA-stimulated phosphorylation of the IR can exhibit significant differences when expressed in different cell types, and that Ser^{1315} is a major PMA-stimulated phosphorylation site on the human IR.

INTRODUCTION

The insulin receptor (IR) is serine phosphorylated in its basal state, and this phosphorylation is increased upon stimulation with insulin, phorbol ester, or forskolin [1–3]. Studies with phorbol ester and forskolin have suggested that serine/threonine kinases, such as protein kinase C (PKC) and cyclic AMP-dependent protein kinase, may regulate the biological activity of the IR. These reports have shown that phorbol ester- and forskolin-induced phosphorylation of the IR correlated with impaired receptor tyrosine kinase activity, increased endocytic trafficking and decreased insulin binding [4–12]. Other studies, however, did not detect any effect of this phosphorylation on the IR's tyrosine kinase activity or insulin binding [2,4,13]. The basis for these conflicting reports on the effect of phorbol ester stimulation on the IR is unknown, and a consensus on the role of PKC in the regulation of IR action has not been reached. Further characterization of phorbol ester-stimulated phosphorylation of IR is necessary to establish the role of PKC in the regulation of its biological activity.

Phosphopeptide analysis of IR has indicated that the receptor contains multiple phorbol ester-stimulated phosphorylation sites [5,14–16]. The major phorbol ester- and PKC-stimulated threonine phosphorylation site on IR is Thr^{1336} [14,15]. (The numbering system for IR is according to that of Ullrich et al. [17].) This Thr^{1336} has also been reported to be the predominant site of insulin-stimulated threonine phosphorylation on the receptor *in vivo* [16]. Study of Chinese hamster ovary (CHO) cells overexpressing both IR and PKC have shown that phorbol ester-stimulated PKC can also increase receptor phosphorylation at Ser^{1293}/Ser^{1294}, a site that was originally identified as an insulin-stimulated serine phosphorylation site *in vitro* by a tightly associated insulin-stimulated serine kinase [18,19]. However, the phosphorylation of Ser^{1293}/Ser^{1294} represents only a small fraction of the total phorbol ester- or insulin-stimulated serine phosphorylation on the IR, and the mutagenesis of these residues had no effect on the receptor's autophosphorylation or tyrosine kinase activity [16]. Thus the major sites of both phorbol ester- and insulin-stimulated serine phosphorylation of the receptor are unknown. Moreover, as expression of Ser/Thr kinases and phosphatases can vary in different cell types, variability in the sites of serine phosphorylation on the IR may occur in different cellular backgrounds.

In this report, the phorbol 12-myristate 13-acetate (PMA)-stimulated phosphorylation of wild-type human IR and a C-terminal truncated mutant ($IR_{\Delta CT}$) was characterized and compared in two different cell types. Tryptic phosphopeptide analysis by Tricine/SDS/PAGE was used to examine the PMA- and insulin-stimulated phosphorylation of IR. This analysis revealed significant differences in the PMA-stimulated phosphorylation of the IRs expressed in normal rat kidney epithelial (NRK) cells compared with CHO fibroblasts. A major site of PMA-stimulated phosphorylation on the IR was identified near its C-terminus at Ser^{1315}. This PMA-stimulated phosphorylation of the IR did not inhibit the insulin-stimulated phosphorylation of the regulatory-domain tyrosines at positions 1146, 1150 and 1151 in intact cells, indicating that the phosphorylation of Ser^{1315} does not inhibit IR tyrosine kinase activity.

MATERIALS AND METHODS

Cell culture and transfection

NRK-52E cells (American Type Cell Culture) were cultured in Dulbecco's modified Eagle's medium (DMEM) containing 5% (v/v) newborn-calf serum (NBCS). NRK cells were co-transfected with human IR cDNA (pSVHIRc) and neomycin-resistant (pSVEneo) plasmids at a ratio of 10:1 by electroporation [20]. The wild-type human IR cDNA used was exon 11 minus

Abbreviations used: FBS, fetal bovine serum; NBCS, newborn-calf serum; WGA, wheat germ agglutinin; TFA, trifluoroacetic acid; DMEM, Dulbecco's modified Eagle's medium; PMA, phorbol 12-myristate 13-acetate; PKC, protein kinase C; IR, insulin receptor; $IR_{\Delta CT}$, C-terminal truncated IR mutant; NRK, normal rat kidney epithelial; CHO, Chinese hamster ovary; TPCK, tosylphenylalanylchloromethane.

* To whom correspondence should be addressed.

[17]. The IR mutant ($IR_{\Delta CT}$), which contained a 43 C-terminal amino acids truncation, has been described previously [21]. NRK cells expressing high levels of IR or $IR_{\Delta CT}$ were isolated by fluorescence-activated cell sorting and cloned. Cells were maintained in DMEM containing 5% (v/v) NBCS and 0.8 g/l G418 (neomycin, Gibco-BRL). CHO-K1 cells transfected with IR and $IR_{\Delta CT}$ were cultured in F-12 medium containing 10% (v/v) fetal bovine serum (FBS) and 0.8 mg/ml G418 and have been characterized previously [22].

Insulin binding

Insulin binding was performed on confluent monolayers of transfected NRK cells cultured on 12-well Costar plates. Cells were bound with 0.1 ng/ml ^{125}I-insulin in the presence of increasing concentrations of unlabelled insulin (Eli Lilly Co., Indianpolis, IN, U.S.A.) in DMEM containing 1% (w/v) BSA at 4 °C for 18 h. Cells were then washed three times with ice-cold PBS and solubilized with 0.1 M NaOH. NRK cells expressed a low level of endogenous rat IRs (< 10000 receptors/cell). Transfection with plasmids containing wild-type and mutant human IR cDNA increased insulin binding by 20-fold over the transfection of cells with only neomycin-resistance plasmid. The CHO cells transfected with IR and $IR_{\Delta CT}$ expressed 1×10^6 IRs/cell [22].

In vitro phosphorylation

CHO/IR and CHO/$IR_{\Delta CT}$ cells were lysed in 50 mM Hepes (pH 7.6), containing 1% (v/v) Triton X-100, 2 mM phenylmethanesulphonyl fluoride and 1 mg/ml aprotinin (Sigma). The soluble fraction was applied to a wheat-germ agglutinin (WGA)–Sepharose column (Sigma) and was eluted with 0.3 M *N*-acetyl-D-glucosamine. The partially purified IR was autophosphorylated in the presence of 17 nM insulin, 5 mM $MnCl_2$ and 100 μM [γ^{32}P]ATP (New England Nuclear) for 30 min at 22 °C.

In vivo phosphorylation

Confluent monolayers of cells in 15-cm-diam. plates were serum starved for 18 h. Cells were then incubated for 2 h in phosphate-free Eagle's minimum essential medium containing 0.3 mCi/ml [^{32}P]Pi (New England Nuclear). Cells were then stimulated with 320 nM PMA for 30 min or 100 ng/ml insulin for 10 min. Labelling was terminated with liquid N_2, and cells were thawed and scraped from the dish with 50 mM Hepes (pH 7.6), containing 1% Triton X-100, 100 mM NaF, 2 mM sodium vanadate, 10 mM sodium pyrophosphate, 1 mg/ml aprotinin, 4 mM EDTA and 2 mM phenylmethanesulphonyl fluoride (Sigma). The cell lysate was centrifuged at 100000 ***g*** for 30 min, and the soluble fraction was bound to WGA–Sepharose and eluted with 0.3 M *N*-acetyl-D-glucosamine. The WGA-purified fraction was treated with 5 μg of monoclonal anti-(human IR) antibody 83-14 (provided by Professor K. Siddle, University of Cambridge, Cambridge, U.K.) at 4 °C for 18 h and immunoprecipitated with pansorbin (Calbiochem) as described [23]. Samples were eluted with Laemmli sample buffer [24] and separated on SDS/7.5% PAGE. Protein was transferred to nitrocellulose (Schleicher and Schuell) and visualized by autoradiography.

Phosphoamino acid analysis

In situ ^{32}P-labelled IR was prepared and transferred to nitrocellulose as described above. Nitrocellulose containing the β-subunit was excised and treated with 0.5% (w/v) polyvinylpyrrolidone (PVP-40) in 100 mM acetic acid for 1 h at 37 °C. The paper was then washed extensively with water and digested for 24 h with 100 μg of tosylphenylalanylchloromethane (TPCK)-treated trypsin (Worthington) in 100 mM NH_4HCO_3, pH 8.2, containing 5% (v/v) acetonitrile. An additional 10 μg of TPCK-treated trypsin was added and the digestion was continued for an additional 24 h. This technique consistently eluted 90–95% of phosphopeptides. The digests were then evaporated in a Speed Vac, partially hydrolysed in 100 μl of 6 M HCl at 110 °C for 2 h, diluted with 1 ml of water and dried. Phosphoamino acid analysis was performed by electrophoresis on Avicel t.l.c. plates (Analtech), as described previously [25,26].

Tryptic phosphopeptide analysis by Tricine/SDS/PAGE

IR separated by SDS/PAGE was transferred to nitrocellulose and the ^{32}P-labelled β-subunit was visualized by autoradiography. The β-subunit was excised and digested with TPCK-treated trypsin in 100 mM $NaHCO_3$, pH 8.2, as described above. The trypsinization was terminated by the addition of double-strength Tricine sample buffer [27] and boiled for 3 min. The phosphopeptides were separated by Tricine/SDS/PAGE, as described by Schägger and von Jagow [27], using a 32-cm-long acrylamide gel consisting of 3% (w/v) acrylamide stacking, 10% separating and 16.5% resolving gels. The gels were sealed with plastic wrap and either exposed to film at −80 °C or to a phosphorimager screen at −20 °C. Autoradiographs were scanned and quantified on a Molecular Dynamics densitometer or phosphorimager. The molecular masses of the phosphopeptides were estimated using Rainbow low-molecular-mass markers (Amersham).

Manual Edman degradation

Tryptic phosphopeptides P2, P3, and 17 were eluted from the gel and dialysed in Spectrapor 1000 tubing against water. Samples were dried in a Speed Vac, dissolved in 50% acetonitrile in H_2O (v/v), and covalently coupled to Sequelon-AA discs (Millipore) with 1-ethyl-3-(3-dimethylaminopropyl)carbodi-imide. Discs were washed extensively with water/trifluoroacetic acid (TFA)/methanol at 22 °C, and TFA at 50 °C. Edman degradation was performed as described by Sullivan and Wong [28]. Briefly, discs were incubated in coupling reagent (methanol/water/triethylamine/phenylisothiocyanate; 7:1:1:1, by vol.) at 55 °C for 10 min, washed with methanol, and the phenylthiohydantoin derivatives were eluted with TFA at 55 °C for 6 min. The discs were washed once with TFA/42.5% phosphoric acid (Sigma) (9:1, v/v) and six times with methanol. The radioactivity released from the discs was monitored by Cerenkov radiation. The fractions were then concentrated in a Speed Vac, spotted on gel-dryer filter paper (Bio-Rad), and exposed to film at −80 °C.

RESULTS

Comparison of PMA- and insulin-stimulated phosphorylation of IR and $IR_{\Delta CT}$ in NRK and CHO cells

Wild-type human IR and a C-terminal-truncated mutant, $IR_{\Delta CT}$, were overexpressed in NRK cells. Scatchard analysis revealed that the NRK transfectants expressed 2×10^5 IRs/cell (results not shown). Screening of multiple clones of NRK/IR and NRK/$IR_{\Delta CT}$ indicated that this was the maximal level of expression which could be obtained in this cell type. Insulin- and PMA-stimulated phosphorylation of the IR and $IR_{\Delta CT}$ expressed in NRK cells was characterized and compared with the phosphorylation of these receptors in CHO cells (CHO/IR and CHO/$IR_{\Delta CT}$). These transfected cells were labelled with [^{32}P]Pi

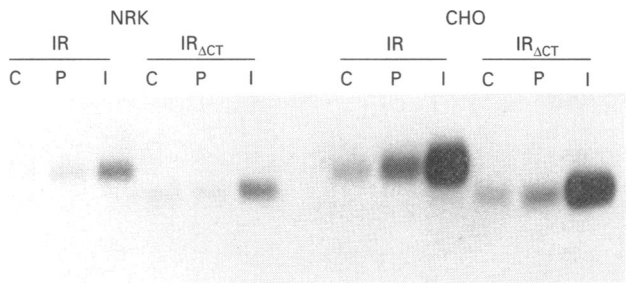

Figure 1 PMA- and insulin-stimulated phosphorylation of IR and $IR_{\Delta CT}$ expressed in NRK and CHO cells

Confluent monolayers of cells were serum starved for 18 h, labelled with 0.3 mCi/ml [^{32}P]P_i in phosphate-free medium for 3 h (C), and stimulated with 320 nM PMA for 30 min (P), or 17 nM insulin for 10 min (I). Labelling was terminated with liquid N_2, and immunoprecipitated IRs were separated by SDS/7.5% PAGE and transferred to nitrocellulose as described in the Materials and methods section. The ^{32}P-labelled β-subunit of the IR was visualized by autoradiography.

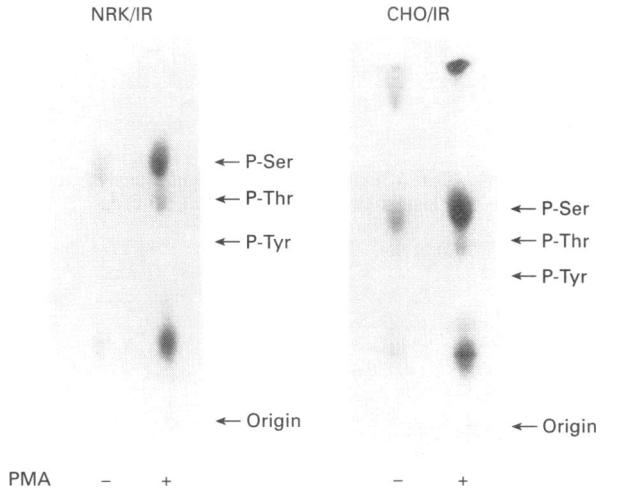

Figure 2 Phosphoamino acid analysis of PMA-stimulated IR

NRK/IR and CHO/IR cells were labelled with [^{32}P]P_i, and the control and PMA-stimulated IRs were isolated as described in Figure 1. ^{32}P-labelled IR β-subunit was trypsinized for 48 h, hydrolysed in 6 M HCl, and phosphoamino acids were separated by thin-layer electrophoresis. ^{32}P-labelled phosphoamino acids were visualized by autoradiography, and identified by comparison with ninhydrin-stained phosphoamino acid standards.

for 2 h and stimulated with 17 nM insulin or 160 nM PMA. The IR was isolated by WGA–Sepharose chromatography, immunoprecipitation, and SDS/PAGE. Incorporation of ^{32}P into IR and $IR_{\Delta CT}$ was quantified by Cerenkov radiation. Insulin-stimulated ^{32}P incorporation into 95 and 90 kDa β-subunits from IR and $IR_{\Delta CT}$ was $452 \pm 170\%$ ($\pm$S.D., $n = 7$) and $465 \pm 161\%$ ($n = 4$) of the unstimulated control in NRK cells and 766 ± 60 ($n = 4$) and 815% ($n = 1$) of control in CHO cells respectively (Figure 1).

Immunoblot analysis of cPKC isoforms expression in these cells was performed as described previously [29]. This analysis demonstrated that both NRK and CHO cells express PKCα and β_2 isoforms, and both isoforms responded to PMA stimulation by translocation from the cytosolic to membranous cellular

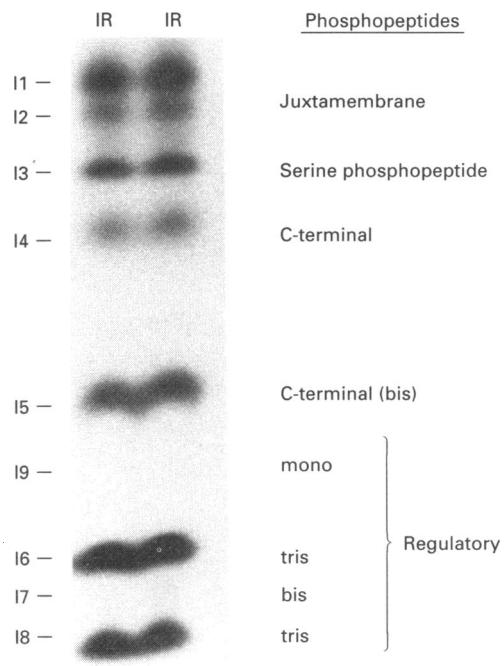

Figure 3 Tricine/SDS/PAGE phosphopeptide map of IR autophosphorylated *in vitro*

Partially purified IR was incubated with 17 nM insulin, 2 mM $MnCl_2$ and 100 μM [γ^{32}P]ATP for 30 min at 22 °C. Labelled IR was immunoprecipitated with antibody 83-14, separated on SDS/7.5% PAGE, transferred to nitrocellulose, and trypsinized as described in the Materials and methods section. Duplicate tryptic phosphopeptide digests were separated by Tricine/SDS/PAGE and visualized by autoradiography. Phosphopeptides I1–I9 have been characterized previously [30].

fractions (results not shown). The PMA-stimulated phosphorylation of IR and $IR_{\Delta CT}$ was compared in these two cell types. Although the fold increase in insulin-stimulated phosphorylation of the IR in CHO cells was greater than in NRK cells, the PMA-stimulated phosphorylation of the IR was similar at $252 \pm 43\%$ ($\pm$S.D., $n = 8$) and $259 \pm 47\%$ ($n = 5$) of the unstimulated control in NRK and CHO cells respectively (Figure 1). The $IR_{\Delta CT}$ mutant was used to determine the role of the C-terminus of the IR in this PMA-stimulated phosphorylation. The basal phosphorylation state of IR and $IR_{\Delta CT}$ unstimulated controls was similar in both NRK and CHO cells. This indicated that the C-terminus does contribute significantly to basal phosphorylation. In NRK cells, PMA did not significantly increase the phosphorylation of $IR_{\Delta CT}$ ($112 \pm 21\%$ of control, $n = 6$; Figure 1). In CHO cells, the PMA stimulation of $IR_{\Delta CT}$ ($168 \pm 17\%$, $n = 3$) was decreased compared with IR, but it was significantly higher than the unstimulated control ($P < 0.05$). This reduction or elimination of PMA-stimulated phosphorylation in $IR_{\Delta CT}$, compared the wild-type IR, suggested that most, or all, of the major PMA-stimulated phosphorylation sites are located within the 43 C-terminal amino acids.

Phosphoamino acid analysis

The phosphoamino acid analysis of the IR in NRK and CHO cells revealed that PMA-stimulated phosphorylation occurred primarily on serine, although a small amount of phosphothreonine was detected (Figure 2). These results agree with previous reports which show that most of the PMA-stimulated

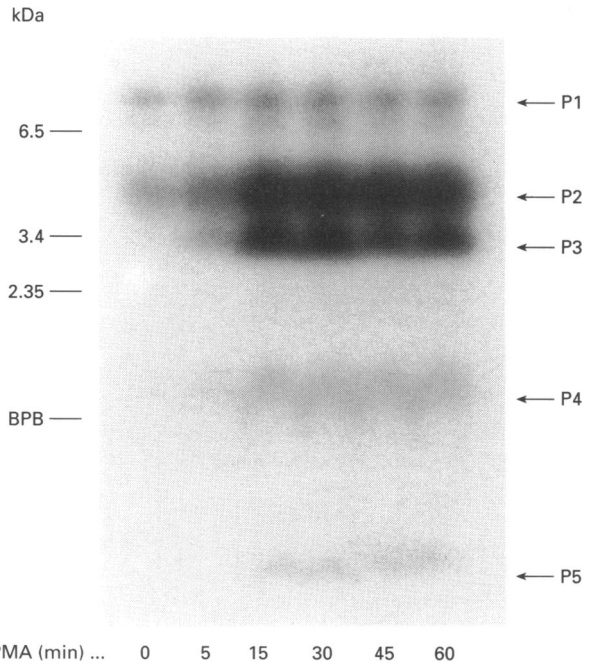

Figure 4 Time course of PMA-stimulated IR phosphorylation on tryptic peptides separated by Tricine/SDS/PAGE

NRK/IR cells, labelled with [^{32}P]P_i were stimulated with 320 nM PMA for the times indicated. Labelled IR was isolated and trypsinized as described in Figure 3. Tryptic phosphopeptides were separated by Tricine/SDS/PAGE and visualized by autoradiography. Molecular masses were estimated with Amersham pre-stained markers and the location of Bromophenol Blue (BPB) is indicated.

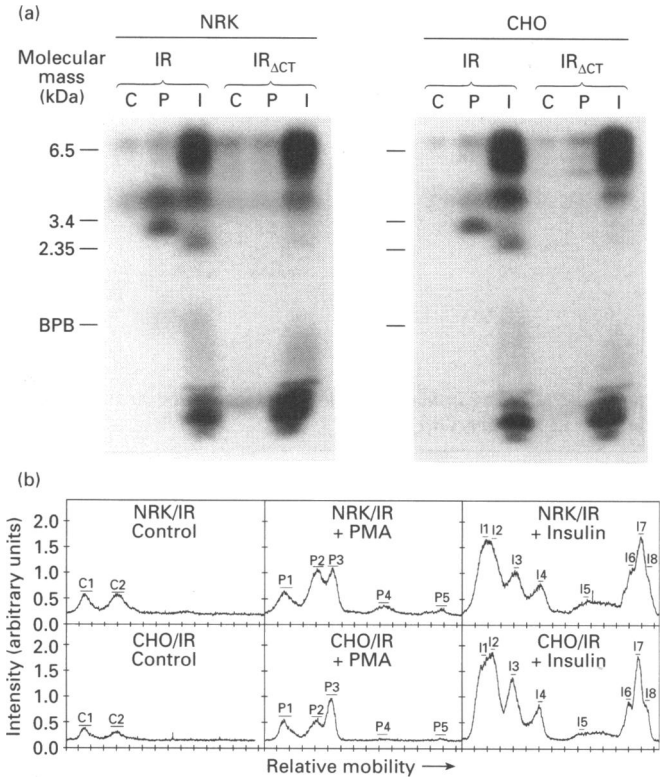

Figure 5 Tricine/SDS/PAGE tryptic phosphopeptide analysis of IR and IR$_{\Delta CT}$ from PMA- and insulin-stimulated NRK and CHO cells

NRK or CHO cells expressing IR or IR$_{\Delta CT}$ were labelled with [^{32}P]P_i, and stimulated with 320 nM PMA for 30 min, or 17 nM insulin for 10 min. The control is the basal phosphorylation of the IR from unstimulated cells. IRs were isolated and trypsinized. (**a**) Tryptic phosphopeptides were separated by Tricine/SDS/PAGE and visualized by autoradiography. (**b**) These autoradiographs were then scanned by laser densitometry and peaks P2 and P3 were integrated. The ratio of P2/P3 was 1.25 ± 0.36 and 0.48 ± 0.26 (mean $\pm$ S.D., $n = 5$) from NRK/IR and CHO/IR cells respectively.

phosphorylation occurs on phosphoserine [4,5,7]. As the PMA-stimulated phosphorylation of IR$_{\Delta CT}$ was reduced or eliminated compared with IR in both cell types (Figure 1), these results indicate that one or more C-terminal serine residue(s) are the major site(s) of PMA-stimulated phosphorylation.

Phosphopeptide analysis of IR by Tricine/SDS/PAGE

The effect of the C-terminal truncation in IR$_{\Delta CT}$ on PMA-stimulated phosphorylation was analysed by tryptic phosphopeptide analysis. PMA- and insulin-stimulated phosphorylation of IR and IR$_{\Delta CT}$ expressed in NRK and CHO cells were compared by phosphopeptide mapping using Tricine/SDS/PAGE [27]. The application of Tricine/SDS/PAGE to tryptic phosphopeptide analysis has allowed the simultaneous analysis of multiple samples, and the side-by-side separation has facilitated the comparison of specific phosphopeptides among separate samples. A description of the tryptic phosphopeptides map from IR autophosphorylated *in vitro* is shown in Figure 3. This map demonstrates that the juxtamembrane, C-terminal, and multiple phosphorylated forms of the regulatory phosphopeptides are resolved with this technique. Densitometric scanning of these peptides allows for quantification of the relative ^{32}P-labelling of these peptides. A detailed analysis of the Tricine/SDS/PAGE phosphopeptide map of wild-type and mutant IRs autophosphorylated *in vitro* and *in vivo* has been described previously [30].

Using Tricine/SDS/PAGE the PMA-stimulated tryptic phosphopeptides, from IR expressed in NRK cells, can be resolved into two major bands, P2 and P3, with apparent molecular masses of 4 and 3 kDa respectively, and three minor bands, P1, P4 and P5 (Figure 4). The time course of PMA stimulation revealed that phosphorylation of P2 and P3 increased to a maximum of approx. 5-fold after 15 min, and remained elevated for at least 1 h. The kinetics of phosphorylation of P2 and P3 were similar (Figure 4). The minor bands at P4 and P5 increased approx. 2-fold. PMA had little or no effect on the phosphorylation of P1, which migrated at 5 kDa. The resolution of these five PMA-stimulated phosphopeptides by this method was comparable with the three to five phosphopeptides resolved by two-dimensional mapping and the four peaks obtained by h.p.l.c. [14,15,19].

Phosphopeptide mapping was used to compare the insulin- and PMA-stimulated phosphorylation pattern of IR and IR$_{\Delta CT}$ in NRK and CHO cells *in vivo* (Figure 5). While IR from both NRK and CHO cells contains the major PMA-stimulated bands at P2 and P3, the relative intensities of these bands are different (Figure 5a). These differences were quantified by the integration of peaks P2 and P3 from the densitometric scans (Figure 5b). The ratio of peak areas for P2/P3 from NRK/IR was 1.25 ± 0.36 ($n = 5$) compared with 0.48 ± 0.26 ($n = 5$) for CHO/IR ($P < 0.01$). Furthermore, the phosphorylation of the minor bands at P4 and P5 was detected in NRK cells but not in CHO cells. Thus while

the fold increase of PMA-stimulated phosphate incorporation in IR was similar in these two cellular backgrounds (Figure 1), the relative phosphorylation of specific tryptic peptides was significantly different.

Tryptic phosphopeptide analysis of insulin-stimulated IR and $IR_{\Delta CT}$ was performed to examine the trypsinization of the IRs from NRK and CHO cells, In contrast with the differences in PMA-stimulated phosphorylation, the phosphopeptide pattern from insulin-stimulated *in vivo* autophosphorylation of IR and $IR_{\Delta CT}$ in these two cell types were identical (Figures 5a and 5b). These tryptic phosphopeptide maps have been characterized previously [30]. The similarities in these phosphopeptide maps from NRK and CHO cells, following the 48 h trypsinization, show that IRs from these two cell types were equally digested. These results indicate that the differences in the tryptic phosphopeptide maps from PMA-stimulated IRs (Figures 5a and 5b, peptides P2 and P3) were due to differences in the distribution of ^{32}P-labelled phosphate, rather than differences in trypsinization.

The major PMA-stimulated phosphopeptides (P2 and P3) were absent in $IR_{\Delta CT}$ from both NRK and CHO cells. The small amount of PMA-stimulated phosphorylation which was observed in $IR_{\Delta CT}$ in CHO cells appeared in phosphopeptide bands not observed in IR (Figure 5a). Thus the C-terminal truncation in $IR_{\Delta CT}$ appears to create additional PMA phosphorylation sites which are not observed in the IR. These results suggested that either the major phosphorylation sites on IR are in the C-terminus, or that the C-terminus is required for the PMA-stimulated phosphorylation elsewhere on the receptor. Previously, we have shown that the juxtamembrane region in the cytosolic domain of the IR is a major site of insulin-stimulated phosphorylation [30]. The role of this region in the PMA-stimulated phosphorylation of the receptor was examined using the mutant $IR_{\Delta 960}$, which contains a deletion from Ala^{954} to Asp^{965} [31]. This deletion removes four serine residues at 955, 956, 962, and 964 [17]. The insulin-stimulated serine phosphorylation of peptides I1 and I2 (Figure 5a) is defective in this mutant [30]. CHO cells expressing $IR_{\Delta 960}$ were labelled with ^{32}P-labelled P_i and stimulated with PMA; tryptic phosphopeptides were analysed by Tricine/SDS/PAGE, as described in Figure 5. The resulting tryptic phosphopeptide map from this receptor contained both P2 and P3, in a ratio similar to that of IR from CHO cells (results not shown). These results demonstrated that P2 and P3 (Figure 5) were not from the juxtamembrane region, and thus were not the same as the major insulin-stimulated phosphorylation previously observed in this region [30]. The PMA-stimulated phosphopeptides were further characterized below by radiosequencing and immunoprecipitation.

Characterization of tryptic phosphopeptides

The PMA- and insulin-stimulated phosphopeptides from *in vivo*-labelled IR were radiosequenced by manual Edman degradation [28]. The peptides P2, P3, and I7 (Figures 5a and 5b) were eluted from the acrylamide gel, dialysed, and sequenced as described previously [30]. The insulin-stimulated peptide I7 from *in vitro*-labelled IR has been shown to correspond to the bis-phosphorylated form of the regulatory domain containing Tyr^{1146}, Tyr^{1150} and Tyr^{1151} [30]. The radiosequence of I7 from *in vivo*-labelled IR revealed that ^{32}P-labelled residues were eluted predominantly from cycles 3 and 7 (Figure 6c). This corresponds to the bis-phosphorylation of Tyr^{1146} and Tyr^{1150} in the regulatory domain. For the PMA-stimulated phosphopeptides, radiolabelled amino acids eluted predominantly during cycles 1 and 3 from P3 and P2 respectively (Figures 6a and 6b). The minor

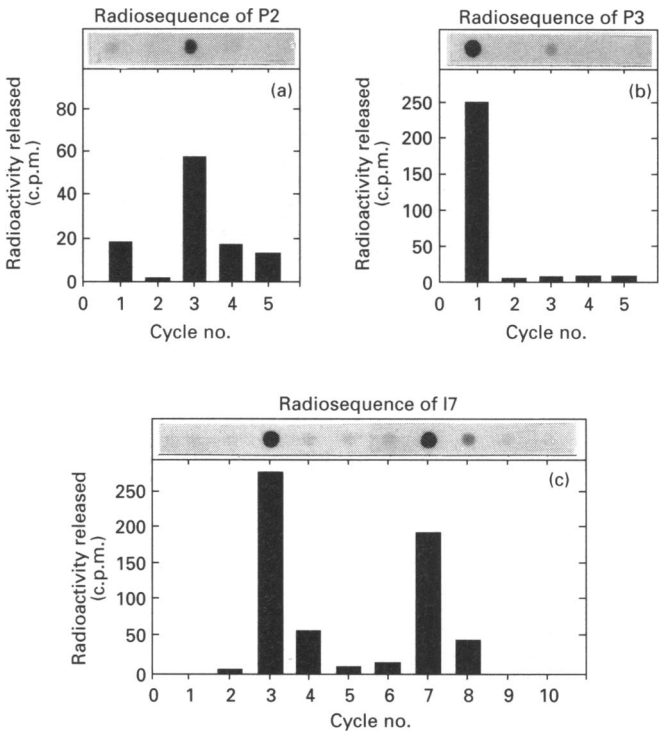

Figure 6 Radiosequencing of tryptic phosphopeptides P2, P3 and I7

Phosphopeptides from PMA- (P2 and P3) and insulin- (I7) stimulated CHO/IR were labelled and separated as described in Figure 5. These peptides were eluted from the Tricine/SDS/PAGE gel, dialysed in Spectapor 1000, covalently coupled to Sequenon AA discs, and manual Edman degradation was performed. The release of radiolabelled amino acids was monitored by counting Cerenkov radiation. The radiosequences of P2, P3, and I7 are shown in (**a**), (**b**) and (**c**) respectively. These eluted fractions were concentrated, spotted on gel-dryer filter paper and visualized by autoradiography at −80 °C. These autoradiographs are shown directly above the bar graph of Cerenkov radiation (c.p.m.).

labelling of these peptides on cycles 3 and 1 from P3 and P2 is probably due to their incomplete separation by Tricine/SDS/PAGE (Figures 5a and 5b). The phosphopeptide P3 appeared to be the major site of phosphorylation on the IR from both CHO and NRK cells. Analysis of the amino acid sequence of the IR revealed that there are two serines at positions 1315 and 1340 which follow a basic amino acid. Tryptic cleavage of the IR would be predicted to generate peptides in which these serines are located at the N-terminus and therefore the residue released by the first cycle of Edman degradation. The identity of the phosphorylated serine was established by immunoprecipitation with a polyclonal antibody (R21-PB8) against residues Ser^{1315} to Lys^{1329} (provided by Dr. R. Smith, Joslin Diabetes Center). This antibody immunoprecipitated IR autophosphorylated *in vitro* and did not precipitate $IR_{\Delta CT}$ (Figure 7a). Twelve 15-cm-diam. plates of CHO/IR were labelled with 1.5 mCi/plate [^{32}P]Pi and were stimulated for 20 min with 160 nM PMA. The ^{32}P-labelled IR was isolated as described in the Materials and methods section, digested for 48 h at 37 °C with TPCK-treated trypsin in the presence of NH_4CO_3, and dried in a Speed Vac. Tryptic phosphopeptides were dissolved in 200 μl of 50 mM Hepes (pH 7.4) containing 150 mM NaF, 0.1 % Triton X-100, 2 mM sodium vanadate, 1 mM phenylmethanesulphonyl fluoride, 0.1 mg/ml aprotinin and 10 mg/ml trypsin inhibitor (Sigma). This mixture was divided into three tubes, treated with normal rat serum or R21-PB8 in the absence or presence of the unlabelled

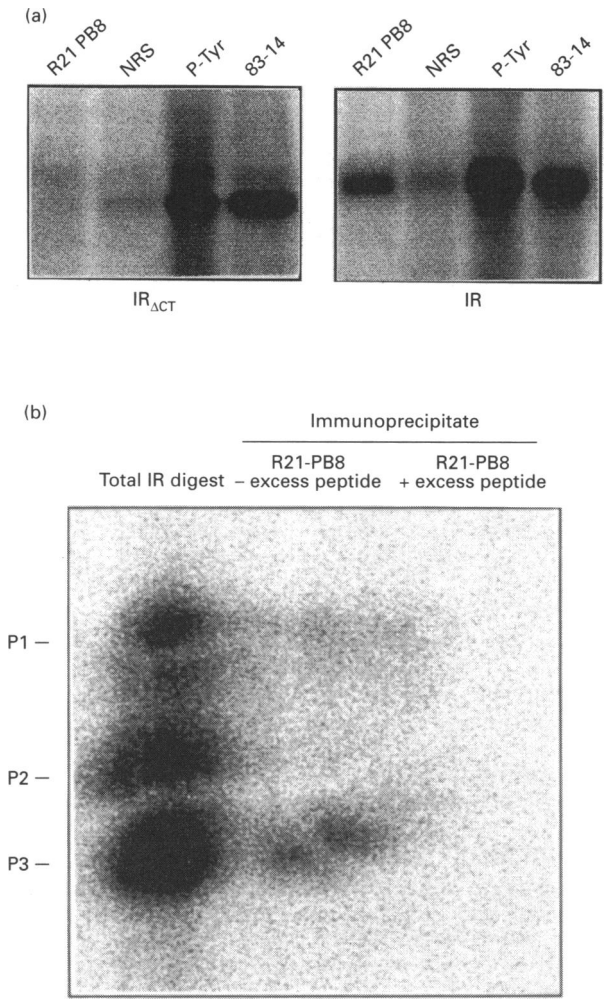

Figure 7 Immunoprecipitation of IR tryptic phosphopeptides from PMA-stimulated CHO/IR cells

(**a**) Partially purified IR and $IR_{\Delta CT}$ from CHO cells were autophosphorylated as described in Figure 3. The ^{32}P-labelled receptors were bound to WGA–Sepharose, and eluted with *N*-acetyl-D-glucosamine to remove excess incorporated [γ-^{32}P]ATP. Labelled IRs were treated with monoclonal anti-IR antibody (83-14), polyclonal anti-phosphotyrosine antibody (P-Tyr), polyclonal antibody against IR sequence Ser^{1315}–Lys^{1329} (R21-PB8), or normal rabbit serum (NRS), and immunoprecipitated with pansorbin. The immunoprecipitates were separated by SDS/PAGE, and visualized with a Molecular Dynamics phosphorimager. (**b**) *In vivo* ^{32}P-labelled IR from PMA-stimulated CHO/IR cells was isolated and digested with trypsin, as described in Figure 5. Aliquots of this tryptic phosphopeptide digest were immunoprecipitated with antibody R21-PB8 in the absence or presence of excess unlabelled peptide containing this sequence. These immunoprecipitates, and a sample containing the total IR tryptic digest, were separated by Tricine/SDS/PAGE and visualized using a Molecular Dynamics phosphorimager. R21-PB8 immunoprecipitated a single bond with mobility corresponding to P3, and the split of this image was due to a crack in the gel.

peptide Asp^{1305} to Lys^{1329} (30 μM) (provided by Dr. W. Heath, Eli Lilly Co., Indianapolis, IN, U.S.A.) at 4 °C for 18 h, and precipitated with pansorbin. The immunoprecipitate was eluted with tricine sample buffer and the Cerenkov radiation was measured. The radioactivity associated with these immunoprecipitates were 155, 36 and 26 c.p.m. for R21-PB8 alone, R21-PB8 with excess unlabelled peptide, and normal rabbit serum respectively. Tricine/SDS/PAGE analysis revealed that R21-PB8 immunoprecipitated a phosphopeptide with an identical mobility to P3, and this peptide was not precipitated in the presence of unlabelled peptide which included Ser^{1315} (Figure 7b). This peptide (P3) was also not precipitated with normal rabbit serum. These results demonstrate that the immunoprecipitation of P3 with R21-PB8 is specific. The other major phosphopeptide (P2) was not precipitated with R21-PB8. Ser^{1315} is the only potential phosphorylation site on the IR which would be consistent with these radiosequence, immunoprecipitation and phosphopeptide-mapping results.

Effect of PMA on the autophosphorylation of IR *in vivo*

The effect of PMA on IR autophosphorylation *in vivo* was examined in both CHO and NRK cells. Cells were labelled with [^{32}P]P_i and stimulated with 160 nM PMA for 15 min, followed by an additional 10 min of stimulation with 17 nM insulin. The IR was isolated, trypsinized and phosphopeptides were analysed by Tricine/SDS/PAGE. IR phosphorylation in the presence of both PMA and insulin displayed a phosphopeptide map which was quantitatively the sum of their effects when added independently (results not shown). The additivity of PMA and insulin on IR phosphorylation suggests that there is little or no overlap in the labelling of the major phosphorylation sites. PMA did not alter the IR autophosphorylation of I6–I8, which have been previously shown to contain bis- and tris-phosphorylation of the regulatory-domain tyrosines Tyr^{1146}, Tyr^{1150}, and Tyr^{1151} (results not shown). These results indicate that PMA-stimulated phosphorylation of the IR at Ser^{1315} does not inhibit the IR's tyrosine kinase activity *in vivo*.

DISCUSSION

The phorbol ester stimulation of cultured cells has been used extensively to examine the potential role of PKC in the regulation of IR phosphorylation and biological activity. While these studies have consistently reported that phorbol esters increase IR β-subunit serine phosphorylation [2,7,14–16], the major sites of this phosphorylation have remained unidentified. In addition, conflicting reports on the effect of phorbol esters on IR autophosphorylation, kinase activity and insulin-binding functions in different cell types and laboratories have made it difficult to generalize on the role of PKC in the regulation of the IR [2,7–13]. If the effects of phorbol ester on the biological activity of the IR is linked to its stimulation of IR phosphorylation, then differences in phosphorylation may contribute to these conflicting results. Although differences in the expression of PKC isoforms, PKC-regulated Ser/Thr protein kinase and Ser/Thr protein phosphatase could result in differences in IR phosphorylation, the significance of the cellular background on the phorbol ester-stimulated phosphorylation is unknown.

In this report, we characterized and compared the PMA-stimulated phosphorylation of the wild-type human IR and a mutant $IR_{\Delta CT}$ expressed in two cell types of different lineage, i.e. an epithelial cell (NRK) and a fibroblast (CHO). This comparison revealed two significant differences in PMA-stimulated IR phosphorylation. First, PMA-stimulated a significant increase in $IR_{\Delta CT}$ β-subunit phosphorylation in CHO cells, but not in NRK cells. Secondly, the distribution of PMA-stimulated phosphate in the β-subunit of the IR was significantly different in these two cell types. In contrast, the tryptic phosphopeptide analysis of insulin-stimulated receptors did not reveal significant differences in receptor autophosphorylation between these cells, indicating that these differences in the PMA-stimulated phosphorylation were not due to differences in the tryptic digestion of the receptors from these two cell types. These results demonstrated that the phorbol ester-stimulated phosphorylation of the IR can

vary significantly in different cell types. The reasons for these differences in IR phosphorylation are not known. Chin *et al.* [19] have shown that overexpression of PKCα, β1, and γ isoforms can increase IR phosphorylation in CHO T cells. Thus the PMA-stimulated phosphorylation of the IR may be a combined effect of multiple PKC isoforms. However, this study also demonstrated that the overexpression of PKCϵ did not enhance the phorbol ester-stimulated phosphorylation of the IR [19], indicating that not all PKC isoforms can contribute to IR phosphorylation. These result are consistent with the differences in substrate specificity of PKC isoforms *in vitro* [32,33]. Of the PKC isoforms which have been demonstrated to increase IR phosphorylation, we only detected the expression of PKCα in NRK and CHO cells. Although expression of PKCβ2 was also detected, it is not known whether this isoform, or any of the other PKC isoforms which have not been examined, can contribute to phorbol ester-stimulated phosphorylation of the IR. Moreover, it is not known whether PKC-stimulated Ser/Thr kinases, such as the MAP kinases [34], contribute to the phorbol ester-stimulated phosphorylation of the IR. Thus further studies are necessary to assess the contribution of PKC isoforms and PKC-activated Ser/Thr kinases to the phorbol ester-stimulated phosphorylation of the IR in different cell types.

Phosphoamino acid analysis of IR from ^{32}P-labelled cells demonstrated that most of the PMA-stimulated phosphorylation occurs on serine. The small amount of phosphothreonine detected is consistent with previous studies, which have reported that Thr^{1336} is a minor phosphorylation site *in vivo* [16]. The comparison of IR and $IR_{\Delta CT}$ expressed in NRK and CHO cells indicated that the C-terminus of the receptor was necessary for normal PMA-stimulated serine phosphorylation. In NRK cells, no PMA-stimulated phosphorylation was observed in $IR_{\Delta CT}$. The phosphorylation of $IR_{\Delta CT}$ which was detected in CHO cells occurred on different phosphopeptides than that from IR, suggesting that the absence of 43 C-terminal amino acids in $IR_{\Delta CT}$ increased the phosphorylation of site(s) which were not labelled in IR. These results on the PMA-stimulated phosphorylation of $IR_{\Delta CT}$ in NRK and CHO cells are different from a report on this receptor in Rat-1 fibroblasts, which found that PMA treatment decreased the basal phosphorylation states of the receptor [35].

Tryptic phosphopeptide analysis of IR with $IR_{\Delta CT}$ from PMA-stimulated cells revealed that the major phosphopeptides in IR (P2 and P3, Figure 5) were absent in the C-terminal mutant. These results suggested that either the 43 amino acids, which are absent in $IR_{\Delta CT}$, contain the major phorbol ester phosphorylation site(s) or that this truncation altered phosphorylation in another location on the receptor. This latter possibility is an important concern since even site-directed mutagenesis of the IR has been shown to alter serine/threonine phosphorylation at another site [30,36]. Thus while mutagenesis of the IR must be consistent with the identification of a phosphorylation site, further direct evidence is necessary to identify a novel phosphorylation site. Analysis of the amino acid sequence of the β-subunit revealed at least 10 serine residues located in a PKC substrate consensus sequence [17,37,38]. Since two of these sites are located within the 43-amino-acid region at the C-terminus, at Ser^{1315} and Ser^{1340}, we examined the potential role of these sites in PMA-stimulated phosphorylation.

The major IR tryptic phosphopeptides from PMA-stimulated CHO cells (P2 and P3) were isolated, and radiosequencing revealed that the first and third residue was phosphorylated respectively. Immunoprecipitation of the ^{32}P-labelled tryptic phosphopeptides with a polyclonal antibody against residues Ser^{1315} to Lys^{1329} immunoprecipitated P3. As Ser^{1315} is the first and only serine residue on this tryptic phosphopeptide, these results demonstrated that Ser^{1315} is a major PMA-stimulated phosphorylation site. The small amount of phosphoamino acid released on the third and first cycle of Edman degradation of P2 and P3 may be due to incomplete separation of these peptides by Tricine/SDS/PAGE. Analysis of sequence adjacent to Ser^{1315} revealed that this site was adjacent to an arginine [17], which is a characteristic of a PKC-recognition sequence [38]. This serine is not in the vicinity of a proline, which is a characteristic of a MAP kinase substrate consensus sequence [34]. While these sequence characteristics are consistent with the direct phosphorylation of Ser^{1315} by PKC, and PKC has been shown to directly phosphorylate the IR *in vitro* [4,14], further studies are necessary to determine the mechanism of PMA-stimulated phosphorylation of Ser^{1315}.

The effect of PMA on the autophosphorylation *in vivo* of the IR was examined in both NRK and CHO cells. Tryptic phosphopeptide mapping of the IR by Tricine/SDS/PAGE resolves the tyrosine phosphorylation domains in the juxtamembrane, regulatory and C-terminal regions [30]. Radiosequencing of the regulatory-domain phosphorylation from IR labelled *in vivo* revealed that Tyr^{1146} and Tyr^{1150} are the major sites for the bis-phosphorylation of this region. Pre-treatment of cells with PMA for 15 min would be expected to increase maximally the PMA-stimulated phosphorylation sites, including Ser^{1315} in peptide P3 (Figure 4). This pretreatment did not inhibit the autophosphorylation of the IR in the regulatory region (I6–I8) or juxtamembrane region (I1 and I2). As the extent of regulatory-domain tyrosine phosphorylation has been shown to regulate the receptor's tyrosine kinase activity [39], these results suggest that PMA does not inhibit the IR tyrosine kinase activity in NRK or CHO cells. These results agree with previous reports which have shown that PMA-stimulated phosphorylation of IR in CHO cells *in vivo* does not inhibit the tyrosine kinase activity of the receptor *in vitro* [13,19].

Radiosequencing of I7 revealed that the bis-phosphorylated form of the regulatory domain is primarily labelled on Tyr^{1146} and Tyr^{1150}. Dickens and Tavare [40] have reported that autophosphorylation of these tyrosines precedes that of Tyr^{1151} in partially purified receptor preparations. Thus the bis-phosphorylation of the regulatory domain *in vivo* is also ordered. This could be due to either a block in the phosphorylation of Tyr^{1151} or the specific dephosphorylation of the tyrosine. The effect of PMA pretreatment on the phosphorylation *in vivo* of the C-terminal tyrosines could not be established because Ser^{1315} resides on the same tryptic peptides as Tyr^{1316} and Tyr^{1322}.

In summary, we have shown that the phorbol ester-stimulated phosphorylation of the IR can significantly vary in different cell types. A major site of this phosphorylation is located in the C-terminus of the receptor at Ser^{1315}. This C-terminal serine phosphorylation did not inhibit insulin-stimulated IR phosphorylation in intact cells. Further studies are necessary to establish the role of the Ser^{1315} phosphorylation on the biological activity of the IR.

We would like to thank Professor K. Siddle and Dr. R. J. Smith for providing us with anti-IR antibodies 83-14 and R21-PB8, and Dr. J. M. Backer for CHO cells expressing $IR_{\Delta 960}$. E.P.F. and P.A.W. were recipients of postdoctoral fellowships from the Juvenile Diabetes Foundation. This work was supported by grants from the National Institutes of Health DK36433 (G.L.K.), and the Diabetes Endocrinology Research Center, DK36836 (G.L.K.).

REFERENCES

1 Kasuga, M., Zick, Y., Blith, D. L., Karlsson, F. A., Haring, H. U. and Kahn, C. R. (1982) J. Biol. Chem. **257**, 9891–9894

2 Takayama, S., White, M. F., Lauris, V. and Kahn, C. R. (1984) Proc. Natl. Acad. Sci. U.S.A. **81**, 7797–7801
3 Statmauer, L. and Rosen, O. M. (1986) J. Biol. Chem. **261**, 3402–3407
4 Bollag, G. E., Roth, R. A., Beaudoin, J., Mochly-Rosen, D. and Koshland, Jr., D. E. (1986) Proc. Natl. Acad. Sci. U.S.A. **83**, 5822–5824
5 Takayama, S., White, M. F. and Kahn, C. R. (1988) J. Biol. Chem. **263**, 3440–3447
6 Roth, R. A. and Beaudoin, J. (1987) Diabetes **36**, 123–126
7 Hachiya, H. L., Takayama, S., White, M. F. and King, G. L. (1987) J. Biol. Chem. **262**, 6417–6424
8 Bottaro, D. P., Bonner-Weir, S. and King, G. L. (1989) J. Biol. Chem. **264**, 5916–5923
9 Thomopoulos, P., Testa, U., Gourdin, M.-F., Hervy, C., Titeux, M. and Vainchenker, W. (1982) Eur. J. Biochem. **129**, 389–393
10 Haring, H., Kirsch, D., Obermaier, B., Ermel, B. and Machicao, F. (1986) J. Biol. Chem. **261**, 3869–3875
11 Blake, A. D. and Strader, C. D. (1986) Biochem. J. **236**, 227–234
12 Grunberger, G. and Gorden, P. (1982) Am. J. Physiol. **243**, E319–E324
13 Coghlan, M. P. and Siddle, K. (1993) Biochem. Biophys. Res. Commun. **193**, 371–377
14 Lewis, R. E., Cao, L., Perregaux, D. and Czech, M. P. (1990) Biochemistry **29**, 1807–1813
15 Koshio, O., Akanuma, Y. and Kasuga, M. (1989) FEBS Lett. **254**, 22–24
16 Tavare, J. M., Zhang, B., Ellis, L. and Roth, R. A. (1991) J. Biol. Chem. **266**, 21804–21809
17 Ullrich, A., Bell, J. R., Chen, E. Y., Herrera, R., Petruzzelli, L. M., Dull, T. J., Gray, A., Coussens, L., Liao, Y.-C., Tsubokawa, M., Mason, A., Seeburg, P. H., Grundfeld, C., Rosen, O. M. and Ramachandran, J. (1985) Nature (London) **313**, 756–761
18 Lewis, R. E., Wu, G. P., MacDonald, R. G. and Czech, M. P. (1990) J. Biol. Chem. **265**, 947–954
19 Chin, J. E., Dickens, M., Tavare, J. M. and Roth, R. A. (1993) J. Biol. Chem. **268**, 6338–6347
20 Shigekawa, K. and Dower, W. J. (1988) Biotechniques **6**, 742–751
21 McClain, D. A., Maegawa, H., Levy, J., Huecksteadt, T., Dull, T. J., Lee, J., Ullrich, A. and Olefsky, J. M. (1988) J. Biol. Chem. **263**, 8904–8912
22 Myers, M. G., Backer, J. M., Siddle, K. and White, M. F. (1991) J. Biol. Chem. **266**, 10616–10623
23 White, M. F., Shoelson, S. E., Keutmann, H. and Kahn, C. R. (1988) J. Biol. Chem. **263**, 2969–2980
24 Laemmli, U. K. (1970) Nature (London) **227**, 680–685
25 Hunter, T. and Sefton, B. M. (1980) Proc. Natl. Acad. Sci. U.S.A. **77**, 1311–1315
26 Kasuaga, M., White, M. F. and Kahn, C. R. (1984) Methods Enzymol. **109**, 6509–6521
27 Schägger, H. and von Jagow, G. (1987) Anal. Biochem. **166**, 368–397
28 Sullivan, S. and Wong, T. W. (1991) Anal. Biochem. **197**, 65–68
29 Oliver, F. J., de la Rubia, G., Feener, E. P., Lee, M.-E, Loeken, M. R., Shiba, T., Quertermous T. and King, G. L. (1991) J. Biol. Chem. **266**, 23251–23256
30 Feener, E. P., Backer, J. M., King, G. L., Wilden, P. A., Sun, X.-J., Kahn, C. R. and White, M. F. (1993) J. Biol. Chem. **268**, 11256–11264
31 Backer, J. M., Kahn, C. R., Cahill, D. A., Ullrich, A. and White, M. F. (1990) J. Biol. Chem. **265**, 16450–16454
32 Marais, R. M., Nguygen, O., Woodgett, J. R. and Parker, P. J. (1990) FEBS Lett. **277**, 151–155
33 Marais, R. M. and Parker, P. J. (1989) Eur. J. Biochem. **182**, 129–137
34 Cobb, M. H., Boulton, T. G. and Robbins, D. J. (1991) Cell Regul. **2**, 965–978
35 Anderson, C. M. and Olefsky, J. M. (1991) J. Biol. Chem. **266**, 27160–21764
36 Tavare, J. M. and Dickens, M. (1991) Biochem. J. **274**, 173–179
37 Kemp, B. E. and Pearson, R. B. (1990) Trends Biochem. Sci. **15**, 342–346
38 Kennelly, P. J. and Krebs, E. G. (1991) J. Biol. Chem. **266**, 15555–15558
39 Wilden, P. A., Kahn, C. R., Siddle, K. and White, M. F. (1992) J. Biol. Chem. **267**, 16660–16668
40 Dickens, M. and Tavare, J. M. (1992) Biochem. Biophys. Res. Commun. **186**, 244–250

Received 4 March 1994; accepted 7 April 1994